

Article

Multi-Year Comparison of Carbon Dioxide from Satellite Data with Ground-Based FTS Measurements (2003–2011)

Ru Miao ^{1,2}, Ning Lu ^{2,*}, Ling Yao ², Yunqiang Zhu ², Juanle Wang ² and Jiulin Sun ²

¹ Institute of Data and Knowledge Engineering, College of Computer and Information Engineering, Henan University, Kaifeng 475004, China; E-Mail: mr1015@henu.edu.cn

² State Key Laboratory of Resources and Environmental Information System, Institute of Geographic Sciences and Natural Resources Research, Chinese Academy of Sciences, Beijing 100101, China; E-Mails: yaoling@reis.ac.cn (L.Y.); zhuyq@reis.ac.cn (Y.Z.); wangjl@igsrr.ac.cn (J.W.); sunjl@igsrr.ac.cn (J.S.)

* Author to whom correspondence should be addressed; E-Mail: ning.robin@gmail.com; Tel.: +86-10-6488-9981; Fax: +86-10-6488-9062.

Received: 16 May 2013; in revised form: 5 July 2013 / Accepted: 8 July 2013 /

Published: 18 July 2013

Abstract: This paper presents a comparison of CO₂ products derived from Scanning Imaging Absorption Spectrometer for Atmospheric Cartography (SCIAMACHY), Greenhouse Gases Observing Satellite (GOSAT) and Atmospheric Infrared Sounder (AIRS), with reference to calibration data obtained using the high-resolution ground-based Fourier Transform Spectrometers (g-b FTS) in the Total Carbon Column Observing Network (TCCON). Based on the monthly averages, we calculate the global offsets and regional relative precisions between satellite products and g-b FTS measurements. The results are as follows: the monthly means of SCIAMACHY data are systemically slightly lower than g-b FTS, but limited in coverage; the GOSAT data are superior in stability, but inferior in systematic error; the mean difference between AIRS data and that of g-b FTS is small; and the monthly global coverage is above 95%. Therefore, the AIRS data are better than the other two satellite products in both coverage and accuracy. We also estimate linear trends based on monthly mean data and find that the differences between the satellite products and the g-b FTS data range from 0.25 ppm (SCIAMACHY) to 1.26 ppm (AIRS). The latitudinal distributions of the zonal means of the three satellite products show similar spatial features. The seasonal cycle of satellite products also illustrates the same trend with g-b FTS observations.

Keywords: greenhouse gases; remote sensing retrievals; carbon dioxide; validation

1. Introduction

Total atmospheric carbon dioxide (CO₂) has increased from approximately 280 to 379 ppm over the past century, due to the burning of fossil fuels for expanding industrial activities [1]. The annual increase in the CO₂ concentration has been as high as 1.9 ppm in the decade from 1995 to 2005, which is higher than the longer term increase of 1.4 ppm per year that has been directly measured for 1960 to 2005 [1]. CO₂ absorbs infrared radiation emitted from the earth's surface, so an increase in CO₂ concentration leads to a rise in atmospheric temperatures. Temperature changes can cause feedback loops that alter CO₂ concentrations by influencing the biosphere [2]. CO₂ and other greenhouse gases also influence tropospheric ozone and water vapor, further increasing their importance to the Earth's radiative budget. Tropical land ecosystems contributed most of the interannual changes in Earth's carbon balance through the 1980s, whereas northern mid- and high-latitude terrestrial ecosystems dominated from 1990 to 1995 [3]. Therefore, CO₂ and other greenhouse gases, such as methane (CH₄), nitrous oxide (N₂O), hydrofluorocarbons (HFCs), perfluorocarbons (PFCs) and sulfur hexafluoride (SF₆), are subject to emissions regulations under the Kyoto Protocol [4]. Research on the greenhouse effect and carbon monitoring require high precision and the long-term measurement of the atmospheric CO₂ concentration. Space-based remote sensing of the CO₂ column-average dry air mole fractions (XCO₂) has the potential to provide observed global constraints on CO₂ fluxes across the surface-atmosphere boundary and to provide insight into the related biogeochemical cycles [5]. As satellite remote sensing technology has developed, a series of satellites that are able to detect CO₂ has been launched. Satellite observations of CO₂ offer new insights into the magnitude of regional sources and sinks and can help overcome the large uncertainties associated with the upscaling and interpretation of data on CO₂ concentration from the Earth's surface [6].

Currently, several satellite instruments can retrieve CO₂ and other greenhouse gas data with significant sensitivity. These include the Scanning Imaging Absorption Spectrometer for Atmospheric Cartography (SCIAMACHY) [7,8] on board the Environmental Satellite (ENVISAT), which was launched in 2002, and the Thermal and Near-infrared Sensor for Carbon Observation (TANSO) [9] on board the Greenhouse Gases Observing Satellite (GOSAT), which was launched in 2009. The Atmospheric Infrared Sounder (AIRS), the Advanced Microwave Sounding Unit (AMSU) and the Humidity Sounder for Brazil (HSB) form an integrated cross-track scanning temperature and humidity sounding system on the Aqua satellite of the Earth Observing System (EOS) [10]. The second Orbiting Carbon Observatory (OCO-2) [11,12] is another satellite designed to observe atmospheric CO₂ in the same spectral region as SCIAMACHY and TANSO in the lower troposphere. The future generation of satellites, such as CarbonSat, which is to be launched in 2019 at the earliest [13–15], will also be able to constrain the parameterization of anthropogenic CO₂ emissions. To study CO₂ sources and sinks, China has launched the Chinese carbon dioxide observation satellite (TanSat) project [16,17]. The TanSat-Chinese will be launched in 2015 and will monitor the CO₂ in the Sun-synchronous orbit.

XCO₂ products retrieved from these satellites have been validated with reference to high-resolution ground-based Fourier Transform Spectrometers (g-b FTS) data and model data. Morino *et al.* [4] validated the GOSAT short wave infrared (SWIR) L2 V01.xx XCO₂ products with the g-b FTS data in nine TCCON sites, and their preliminary findings were that the difference between the GOSAT XCO₂ data and the g-b FTS data was -8.85 ± 4.75 ppm or $-2.3 \pm 1.2\%$. These biases and standard deviations are somewhat higher than those of other validations [5,6,18]. Yoshida *et al.* [19] identified and corrected the Version 01.xx GOSAT XCO₂ products using a revised version of the retrieval algorithm (Version 02.xx). The improved retrieval algorithm had much smaller biases and standard deviations (-1.48 ppm and 2.10 ppm) for XCO₂ than did Version 01.xx. Inoue *et al.* [20] used two approaches to validate the GOSAT XCO₂ products (Version 02.00) with aircraft measurement data. Both methods indicated that the Version 02.00 of GOSAT XCO₂ products were improvements over the previous Version, and the bias was 1–2 ppm, with a standard deviation of 1–3 ppm. Schneising *et al.* [21,22] compared SCIAMACHY XCO₂ data to g-b FTS measurements and model results (CarbonTracker XCO₂) for the period from 2003 to 2009. The relative accuracy was 1.14 ppm relative to TCCON and 1.20 ppm relative to CarbonTracker. Wang *et al.* [23] analyzed SCIAMACHY XCO₂ data levels in China and found that the largest peak-to-trough amplitude of SCIAMACHY was approximately 16 ppm during 2003–2005 and that peaks occurred in the spring, with the trough in winter or autumn. Bai *et al.* [24] validated the AIRS XCO₂ products from 2003 to 2008 using five ground-based stations located throughout the world. The correlation coefficients between AIRS and the other five ground stations were greater than 0.77, with a monthly mean difference of $\sim 0.62 \pm 3.0$ ppm. The average concentration of atmospheric CO₂ was higher in the Northern Hemisphere than in the Southern Hemisphere, with the approximately 2 ppm per year of annual growth in China.

These XCO₂ products have been validated with g-b FTS data and model data, but there are some gaps in these comparisons. These XCO₂ products have been validated individually, but we do not know the differences among the XCO₂ values retrieved from the three sensors (SCIAMACHY, AIRS and GOSAT). Therefore, we have no gauge of which sensors are more precise under what circumstances; additionally, we do not know the differences among these satellite products for different regions. In this paper, the satellite products of GOSAT, SCIAMACHY and AIRS are compared with the reference calibrated data obtained using g-b FTS in the TCCON sites from 2003 to 2011. Through these comparisons, we try to explain why the validations of satellite products differ, to understand the different retrieval methods of the satellite products and to give an overall evaluation. Such a comparison is a prerequisite to evaluating the precision of each product and the suitability for their use in different conditions.

The three sets of satellite data are described in Section 2, where we present an overview of these projects and compare these satellite data sets. Reference data measured with g-b FTS and comparison methods are described in Section 3. The precision analysis of the satellite data products and the preliminary comparison to the reference data are presented in Section 4, where we also analyze the spatial distribution feature, linear trend and seasonal cycle using monthly mean data. The discussion and conclusions follow.

2. Satellite Data Sets

2.1. TANSO on GOSAT

GOSAT was launched on 23 January 2009, by the Japanese Space Agency. The GOSAT Project is a joint effort of the Ministry of the Environment (MOE), the National Institute for Environmental Studies (NIES) and the Japan Aerospace Exploration Agency (JAXA) with the investment of 20 billion Japanese yen [25]. The GOSAT Project primarily estimates the emission and absorption of greenhouse gases on a subcontinental scale. It flies at a 666 km altitude and completes an orbit in approximately 100 min, with an equator crossing time of approximately 1:00 a.m. local time. Its mission is to provide global measurements of total column XCO₂ and XCH₄ from the short wave infrared bands, and it returns to observe the same point on Earth every three days. The instrument on board the satellite is the Thermal and Near-infrared Sensor for Carbon Observation (TANSO), which is composed of two subunits: the Fourier Transform Spectrometer (FTS) and the Cloud and Aerosol Imager (CAI).

Carbon observation is made by an FTS that covers 0.75–14.3 μm [26]: band 1 spans 0.758–0.775 μm (12,900–13,200 cm⁻¹) with 0.37 cm⁻¹ or better spectral resolution, and bands 2–4 span 1.56–1.72, 1.92–2.08 and 5.56–14.3 μm (5,800–6,400 cm⁻¹, 4,800–5,200 cm⁻¹ and 700–1,800 cm⁻¹) respectively, with 0.26 cm⁻¹ or better spectral resolution. The TANSO instantaneous field of view is approximately 15.8 milliradians, corresponding to a nadir footprint diameter of approximately 10.5 km at sea level. The nominal single-scan data acquisition time is 4 s.

XCO₂ and XCH₄ are retrieved from the 1.6 μm CO₂ absorption band and the 1.67 μm CH₄ absorption band using the optimal estimation method [27]. The retrieval algorithm for XCO₂ and XCH₄ is described in Yoshida [28]. It consists of three parts: screening data suitable for the retrieval analyses, optimal estimation of gaseous column abundances and examination of the retrieval quality to exclude low-quality and/or aerosol-contaminated results. Most of the random errors in retrieval come from instrumental noise, while the interference error due to auxiliary parameters is relatively small. GOSAT Level 2 products are evaluated against high-precision data that are obtained independently using ground-based or aircraft observations. GOSAT Level 3 products are generated by interpolating and extrapolating the Level 2 products and can be used to estimate the global distribution of greenhouse gas concentrations. The Level 2 products indicate the analytical value of the amount of greenhouse gas observed at a specific observation point at a specific observation time, and Level 3 products provide a monthly global distribution of greenhouse gases.

2.2. SCIAMACHY on ENVISAT

SCIAMACHY, on board the European environmental satellite, was launched into a Sun-synchronous orbit in a descending node and has an equator crossing time of 10:00 a.m. local time. Its wavelength coverage is from 240 nm to 2,380 nm, with eight observation channels that measure reflected, backscattered and transmitted solar radiation at moderately high spectral resolution (0.2–1.4 nm) in the spectral region [29,30]. The Weighting Function Modified Differential Optical Absorption Spectroscopy (WFM-DOAS) algorithm [31,32], which was produced by the University of Bremen, is an important improvement to the standard DOAS algorithm. The global long-term SCIAMACHY greenhouse gas results for validation are obtained using v2 (v2.1 XCO₂) of the

scientific retrieval algorithm, WFM-DOAS, that was introduced by Schneising *et al.* [21], which is based on a fast look-up table scheme. WFM-DOAS is a least-squares method based on scaling (or shifting) pre-selected atmospheric vertical profiles. XCO₂ is derived by normalizing the CO₂ columns with the simultaneously retrieved oxygen columns from the O₂ A-band. The monthly average concentration data for XCO₂ from January 2003 to December 2009 were retrieved from SCIAMACHY nadir observation mode L1c data combined with the WFM-DOAS algorithm.

The overall precision and bias of the XCO₂ are estimated to be close 1.0% and < 4.0% [33]. The averaging daily standard deviations of the retrieved XCO₂ at different locations are approximately 5.4 ppm (1.4%). Reuter *et al.* [34] validated the XCO₂ retrieved from Bremen Optimal Estimation DOAS algorithm by comparing them with g-b FTS measurements and with CT2009 from 2006 to 2010. The single-measurement precision is no more than 3 ppm, and the year-to-year increase varies between 1.88 ± 0.44 and 2.30 ± 0.03 ppm per year.

2.3. AIRS on Aqua

AIRS is designed to meet the requirements of the NASA Earth Science Enterprise climate research programs and the operational weather-forecasting plans of the National Oceanic and Atmospheric Administration. It is a nadir cross-track scanning infrared spectrometer on the second Earth Observing System [35] Aqua spacecraft, which flies at an altitude of approximately 705 km polar orbit. The sensor on board the satellite has 2,378 channels that cover three spectral regions from 649 to 2,674 cm⁻¹ (649–1,136, 1,217–1,613 and 2,169–2,674 cm⁻¹). It crosses the equator at approximately 1:30 a.m. and 1:30 p.m. local time, resulting in near global coverage twice a day [36]. The instrument field of view is 1.1°, corresponding to a nadir footprint of 13.5 km on the surface, and the scan angles are ±48.95° [10]. AIRS can produce cloud cleared radiance for approximately 60% of the 324,000 FORs (field of regards) per day.

The Version 5 Level 2 retrieval algorithm (V5) that is used to retrieve these products assumes a global average linear time-varying CO₂ climatology throughout the atmosphere [37]. The CO₂ transport model is an atmospheric four-dimensional variational data assimilation system, which is a practical formulation of Bayesian estimation theory [38]. AIRS products meet the criteria identified by the National Research Council for climate data records. XCO₂ retrieved from AIRS uses two thermal infrared strong absorption bands, which correspond to low and mid-high sensitivities to tropospheric concentration.

2.4. Comparisons among Three Satellite Data Sets

For long-term comparison with g-b FTS data, we use the monthly mean data from the satellite products. The global monthly average XCO₂ data for GOSAT (L3 SWIR v01.xx) come from the NIES GOSAT website (http://www.gosat.nies.go.jp/index_e.html) from the period of April 2009 to December 2011, with a sampling grid of 2.5° × 2.5°. The global monthly average XCO₂ data for SCIAMACHY (L3 WFM-DOAS v2.2) come from the SCIAMACHY/WFM-DOAS research team at Germany's University of Bremen (http://www.iup.uni-bremen.de/sciamachy/NIR_NADIR_WFM_DOAS/) for the period of January 2003 to December 2009, with a sampling grid of 0.5° × 0.5°. The global monthly average XCO₂ data for AIRS (L3 AIRS+AMSU v5) come from the NASA AIRS website

(<http://disc.sci.gsfc.nasa.gov/AIRS/data-holdings>) in the period of January 2002 to December 2011, with a sampling grid of $2^\circ \times 2.5^\circ$.

The comparison of the performance of the satellite sensors for the three on-orbit satellites, GOSAT, SCIAMACHY and AIRS, are listed in Table 1. There are two salient features of the various CO₂ observation parameters: (1) a wide band range with high spectral resolution, but relatively lower spatial resolution; and (2) nadir observation mode in all sensors, except SCIAMACHY, which uses a variety of observation mode. The boundary layer observation mode of SCIAMACHY has higher vertical resolution and greater sensitivity, and can obtain the higher precision atmospheric vertical profile of the troposphere and stratosphere [39]. Some characteristics of the CO₂ absorption band and other necessary spectral characteristic channel of retrieval parameters are all include in the spectral range. AIRS mainly uses the thermal infrared absorption band for CO₂ near 4.3 μm and 1.5 μm , which is most sensitive to CO₂ in the low and mid-high layers. SCIAMACHY primarily uses the short-wave infrared weak absorption band of CO₂ near 1.58 μm , which is most sensitive to CO₂ near the ground. In addition to these, GOSAT uses the short wave infrared weak absorption band of CO₂ near 2.06 μm , which covers the most general CO₂ characteristic bands in the current monitoring of CO₂ and has great significance for CO₂ detection band selection in future platforms [40].

Table 1. The satellite sensors performance parameters of Greenhouse Gases Observing Satellite (GOSAT), Scanning Imaging Absorption Spectrometer for Atmospheric Cartography (SCIAMACHY) and Atmospheric Infrared Sounder (AIRS). TANSO, Thermal and Near-infrared Sensor for Carbon Observation; FTS, Fourier Transform Spectrometer; CAI, Cloud and Aerosol Imager; ENVISAT, Environmental Satellite.

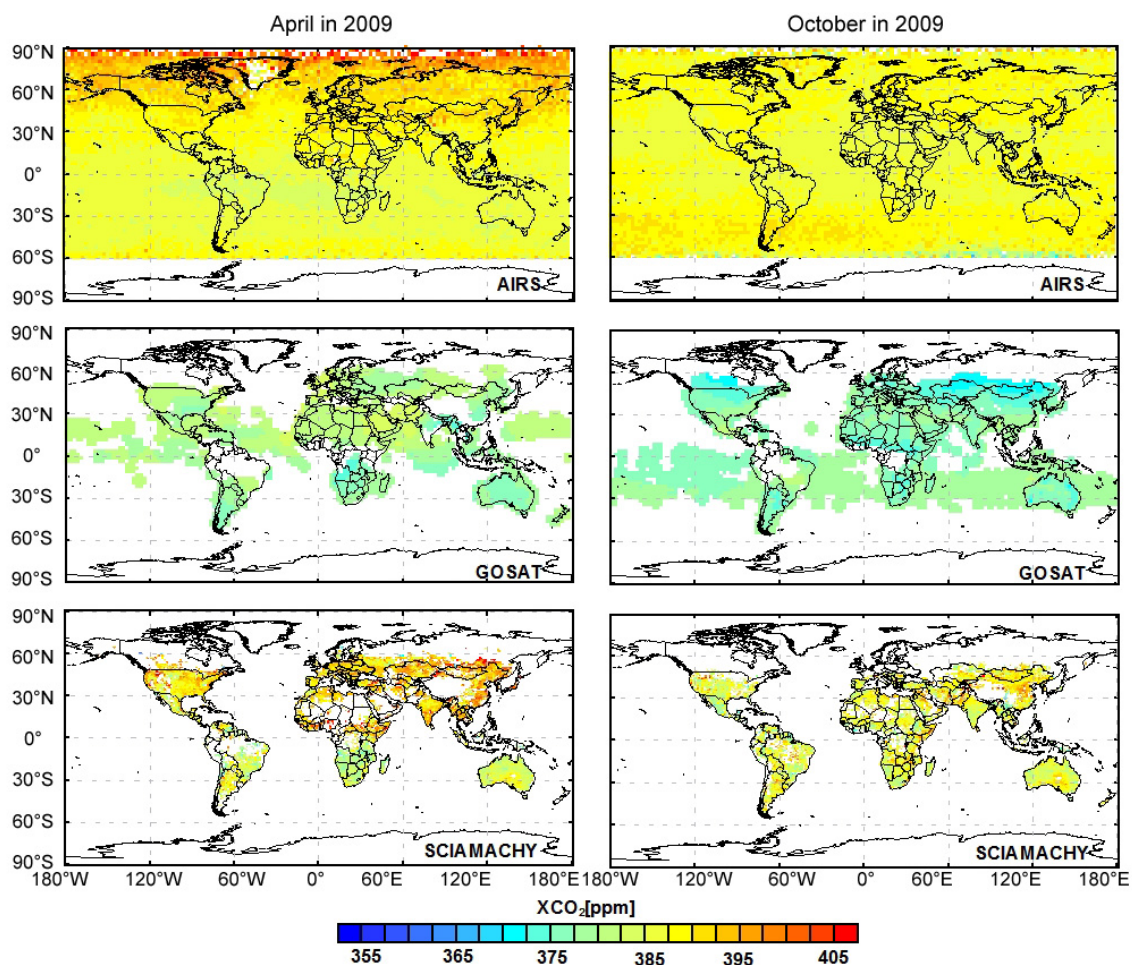
Sensors	GOSAT-TANSO	SCIAMACHY	AIRS
Onboard satellite	GOSAT	ENVISAT	Aqua
Orbital altitude (km)	666	799.8	705.3
Spatial resolution (km)	10.5	30 × 60	13.5
Spectral region (μm)	0.75–14.3	0.24–2.38	3.7–15.4
Spectral resolution (cm^{-1})	0.2	1.0–7.8	0.55–2.0
Detecting instrument	FTS and CAI	8 channel grating spectrometer	grating spectrometer
Observation mode	nadir, flare, target	limb, nadir	nadir
Signal to noise ratio (dB)	120 (1.56~1.72 μm)	<100 (1.57 μm)	2,000 (4.2 μm)
	120 (1.92~2.08 μm)		1,400 (3.7~13.6 μm) 800 (13.6~15.4 μm)

Figure 1 shows the global XCO₂ distribution of the monthly averaged AIRS, GOSAT and SCIAMACHY, gridded in 2° by 2.5° bins, 2.5° by 2.5° bins and 0.5° by 0.5° in April and October, 2009, respectively. For AIRS, data covering almost the entire surface of the Earth are obtained for 60°S to 80°N in both April and October. For GOSAT, terrestrial data are obtained mainly for 10 – 60°N and 15 – 45°S in April and for 10 – 50°N and 0 – 50°S in October. Data over the oceans are retrieved from 10°S to 30°N in April and from 40°S to 10°N in October by observing the specular reflection of sunlight in the direction of sunlight.

In Figure 1, we can see that the SCIAMACHY data are confined to the land. The GOSAT data cover the ocean and some nearshore sea areas within the latitudes of 40°S – 40°N . The coverage of

AIRS data has greatly improved; with the exception of latitudes to the south of 60°S near the arctic pole point, the monitoring scope of AIRS covers most of the world. The global data coverage for a single month for the three satellites varies: the SCIAMACHY products cover only 8–20%, GOSAT products improve that figure to 32–44% and AIRS products cover 95%, which provides an obvious advantage compared to the other types of satellite data.

Figure 1. The global XCO₂ concentration distribution retrieved from AIRS, GOSAT and SCIAMACHY in April 2009 and in October 2009.



The spatial differences in XCO₂ between three sensor measurements are mainly due to the product selection for validation. The GOSAT XCO₂ data products shown here are filtered for aerosol optical depth less than 0.5. As a plane-parallel atmosphere is assumed in the retrieval, data with solar zenith angles greater than 70 degrees are not processed, and data over high mountain ranges, such as the Rockies, the Andes and the Himalayan mountains, are removed [4]. SCIAMACHY measurements over the ocean are filtered out, because of the lower surface reflectance. In order to get larger global data coverage scale, the AIRS XCO₂ product lost some accuracy in the product process. Thermal infrared band sensitive channels used in the AIRS XCO₂ product are superior to the near-infrared wave band for the ocean detection ability of CO₂. Therefore, AIRS has stronger detection ability for CO₂ over the ocean compared with the other kinds of satellites.

3. Reference Data and Comparison Methodology

3.1. g-b FTS Data for Satellite Product Validation

TCCON is a global network of ground-based high resolution FTS that record direct solar spectra in the near-infrared spectral region [41]. The g-b FTS data are calibrated using airborne *in situ* measurements and apply single scaling factors for each species to all sites consistently. The precision of g-b FTS measurements of XCO₂ are better than 0.2% under clear skies [42–45]. They provide validation data for column-averaged satellite data with accurate and precise column-averaged abundances of CO₂ and CH₄.

To ensure data comparability, all TCCON sites use similar instrumentation (Bruker IFS 125/HR for all sites in this study) and a common retrieval algorithm based on scaling *a priori* profiles by least-squares fitting [22]. The CO₂ *a priori* profiles are derived from an empirical model based on GLOBALVIEW *in situ* data and extended to the stratosphere using an age of air relationship [46].

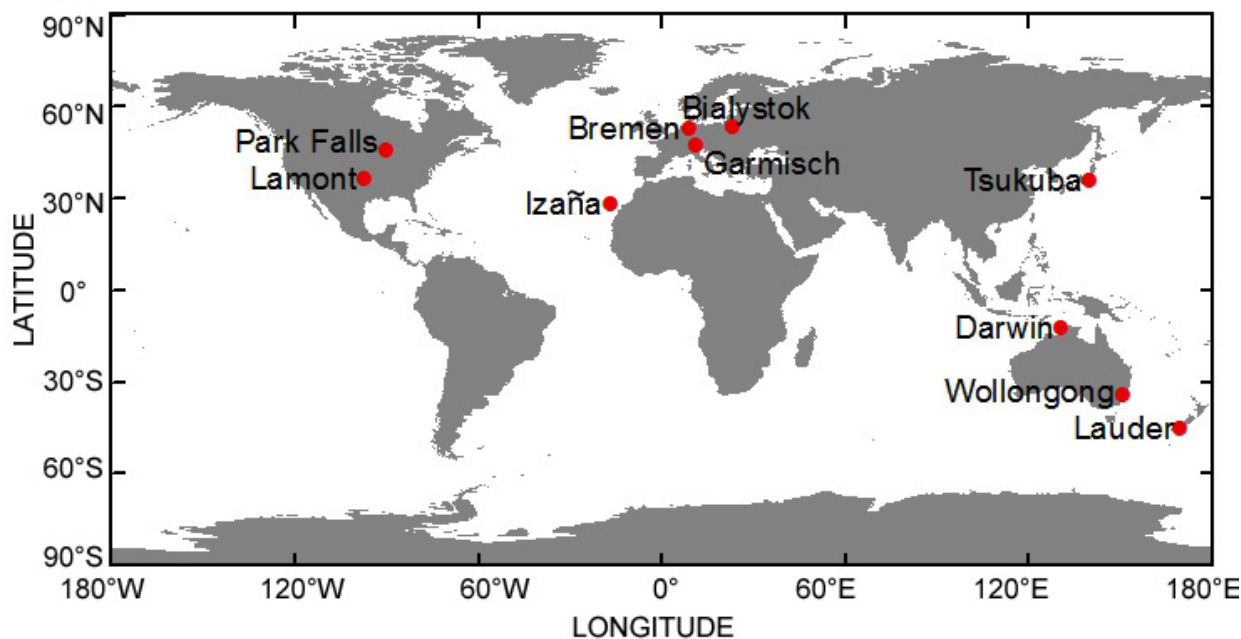
The comparison was performed at the following TCCON sites: Białystok (Poland), Bremen (Germany), Garmisch (Germany), Park Falls (USA), Lamont (USA), Tsukuba (Japan), Izaña (Spain), Darwin (Australia), Wollongong (Australia) and Lauder (New Zealand). The g-b FTS data from the ten TCCON sites are used in this analysis. Table 2 summarizes the spatial coordinates of those stations. Figure 2 shows the locations of the TCCON sites that are used in this paper.

Table 2. TCCON sites used for satellite products validation.

Site	Country	Coordinate [Latitude, Longitude]	Altitude [m a.s.l.]	Reference
Białystok	Poland	53.23 °N, 23.02 °E	180	[47]
Bremen	Germany	53.103 °N, 8.85 °E	30	
Garmisch	Germany	47.47 °N, 11.06 °E	746.6	[48]
Park Falls	USA	45.94 °N, 90.27 °W	442	[42]
Lamont	USA	36.60 °N, 97.48 °W	320	[41, 44]
Tsukuba	Japan	36.05 °N, 140.12 °E	31	[49]
Izaña	Spain	28.31 °N, 16.49 °W	2,373	
Darwin	Australia	12.42 °S, 130.89 °E	32	[43]
Wollongong	Australia	34.41 °S, 150.87 °E	30	
Lauder	New Zealand	45.04 °S, 169.68 °E	370	

For each TCCON site, an XCO₂ time series from SCIAMACHY, GOSAT, AIRS and g-b FTS was generated for validation and comparison. AIRS data are available for the entire analyzed time period ranging from 2003 to 2011, whereas SCIAMACHY and GOSAT data are available for certain subperiods, *i.e.*, 2003 to 2009 and 2009 to 2011, respectively. Similarly, g-b FTS data are also available for certain subperiods depending on the site (Park Falls and Lauder since 2004, Darwin since 2005, Bremen and Izaña since 2007, Tsukuba, Lamont and Wollongong since 2008 and Białystok and Garmisch since 2009). However, in Izaña, there are too few WFM-DOAS retrievals that passed the quality filter for a statistically significant comparison, so no SCIAMACHY data are available for the analyzed time period. Therefore, the comparison between satellite products and g-b FTS data is presented not only for the entire analyzed time period, but also for two subperiods, from January 2003 to December 2008, and January 2009 to December 2011. Thereby, we can see whether these products are stable in different periods of performance.

Figure 2. The locations of TCCON sites used in this paper are indicated by red dots.



3.2. Comparison Methodology

The monthly mean values of the g-b FTS data are calculated from the total of the daily TCCON site measurements divided by the number of days of the month. Additionally, no corrections (on the *a priori* or on the averaging kernel) have been considered in the manuscript. The time series of the satellite product's individual mean volume mixing ratio (vmr) in the i th TCCON site is defined as x_i^r , and the corresponding monthly mean g-b FTS value is defined as x_i^{FTS} . Accordingly, the relative difference between the selected satellite products and the g-b FTS data is:

$$\frac{x_i^r - x_i^{FTS}}{x_i^{FTS}} \quad (1)$$

The mean difference between satellite products and g-b FTS data can be calculated using the following formula:

$$d = \frac{\sum_{i=1}^n (x_i^r - x_i^{FTS})}{n} \quad (2)$$

where n is the number of pairs of satellite product data and corresponding g-b FTS data. The standard deviation of these differences is calculated as $s = std(x_i^r - x_i^{FTS})$, and the correlation coefficient between satellite data and g-b FTS data is $r = correlation(x_i^r - x_i^{FTS})$. The global offset is the averaged d over all TCCON sites in this paper. The regional precision relative to the reference g-b FTS data is the averaged s , and the relative accuracy is the standard deviation of d .

4. Results

4.1. Regional Precision and Relative Accuracy

The XCO₂ results for each satellite product are listed in Table 3 for each site, showing the mean differences (d) to g-b FTS, the standard deviations of the differences (s) and the correlation coefficients (r) for the analyzed time period and the two subperiods. Table 4 summarizes the results.

The two subperiods are January 2003 to December 2008, and January 2009, to December 2011. The corresponding monthly time series and relative differences are depicted in Figures 3 and 4 for the entire analyzed time period for Bialystok, Bremen, Garmisch, Park Falls, Lamont, Tsukuba, Izaña, Darwin, Wollongong and Lauder.

Table 3. XCO₂ validation and comparison results for three satellite products based on monthly data for the entire analyzed time period and for two subperiods from January 2003, to December 2011. Shown are the number of coincident months (*n*) of data availability for satellite data and the comparative data set, the mean difference (*d*) to ground-based (g-b) FTS, the standard deviation of the difference (*s*) and the correlation coefficients (*r*) for the analyzed sites. The global offset is the average mean difference over all sites, the regional precision relative to the reference is the average standard deviation of the difference and the relative accuracy is the standard deviation of the mean difference.

Location		GOSAT-FTS		SCIAMACHY-FTS		AIRS-FTS		
		09–11	03–08	09–11	03–11	03–08	09–11	03–11
Bialystok (53.23°N, 23.02°E)	<i>n</i>	9	0	5	5	0	23	23
	<i>d</i> [ppm]	−7.25	-	−0.83	−0.83	-	−0.83	2.27
	<i>s</i> [ppm]	2.47	-	5.80	5.80	-	5.80	3.48
	<i>d</i> (100%)	−1.87	-	−0.22	−0.22	-	−0.22	0.59
	<i>s</i> (100%)	0.63	-	1.50	1.50	-	1.50	0.90
	<i>r</i>	0.74	-	0.69	0.69	-	0.42	0.42
Bremen (53.10°N, 8.85°E)	<i>n</i>	11	6	5	11	17	24	41
	<i>d</i> [ppm]	−6.74	2.22	1.71	1.99	−0.09	2.82	1.61
	<i>s</i> [ppm]	1.92	2.16	7.08	5.04	2.28	2.69	2.91
	<i>d</i> (100%)	−1.74	0.57	0.44	0.51	−0.02	0.73	0.42
	<i>s</i> (100%)	0.49	0.56	1.84	1.31	0.59	0.70	0.75
	<i>r</i>	0.84	0.78	0.08	0.29	0.46	0.59	0.52
Garmisch (47.48°N, 11.06°E)	<i>n</i>	15	0	3	3	0	21	21
	<i>d</i> [ppm]	−7.24	-	−7.06	−7.06	-	2.38	2.38
	<i>s</i> [ppm]	2.31	-	7.84	7.84	-	3.10	3.10
	<i>d</i> (100%)	−1.87	-	−1.82	−1.82	-	0.61	0.61
	<i>s</i> (100%)	0.59	-	2.03	2.03	-	0.80	0.80
	<i>r</i>	0.55	-	−0.87	−0.87	-	0.22	0.22
Park Falls (45.94°N, 90.27°W)	<i>n</i>	14	30	5	35	47	26	73
	<i>d</i> [ppm]	−4.63	−4.55	−0.21	−3.93	−0.30	5.21	1.66
	<i>s</i> [ppm]	3.21	3.74	2.32	3.88	4.27	3.84	4.90
	<i>d</i> (100%)	−1.19	−1.19	−0.05	−1.03	−0.07	1.36	0.43
	<i>s</i> (100%)	0.83	0.98	0.60	1.01	1.11	1.01	1.28
	<i>r</i>	0.53	0.71	0.87	0.74	0.26	0.32	0.44

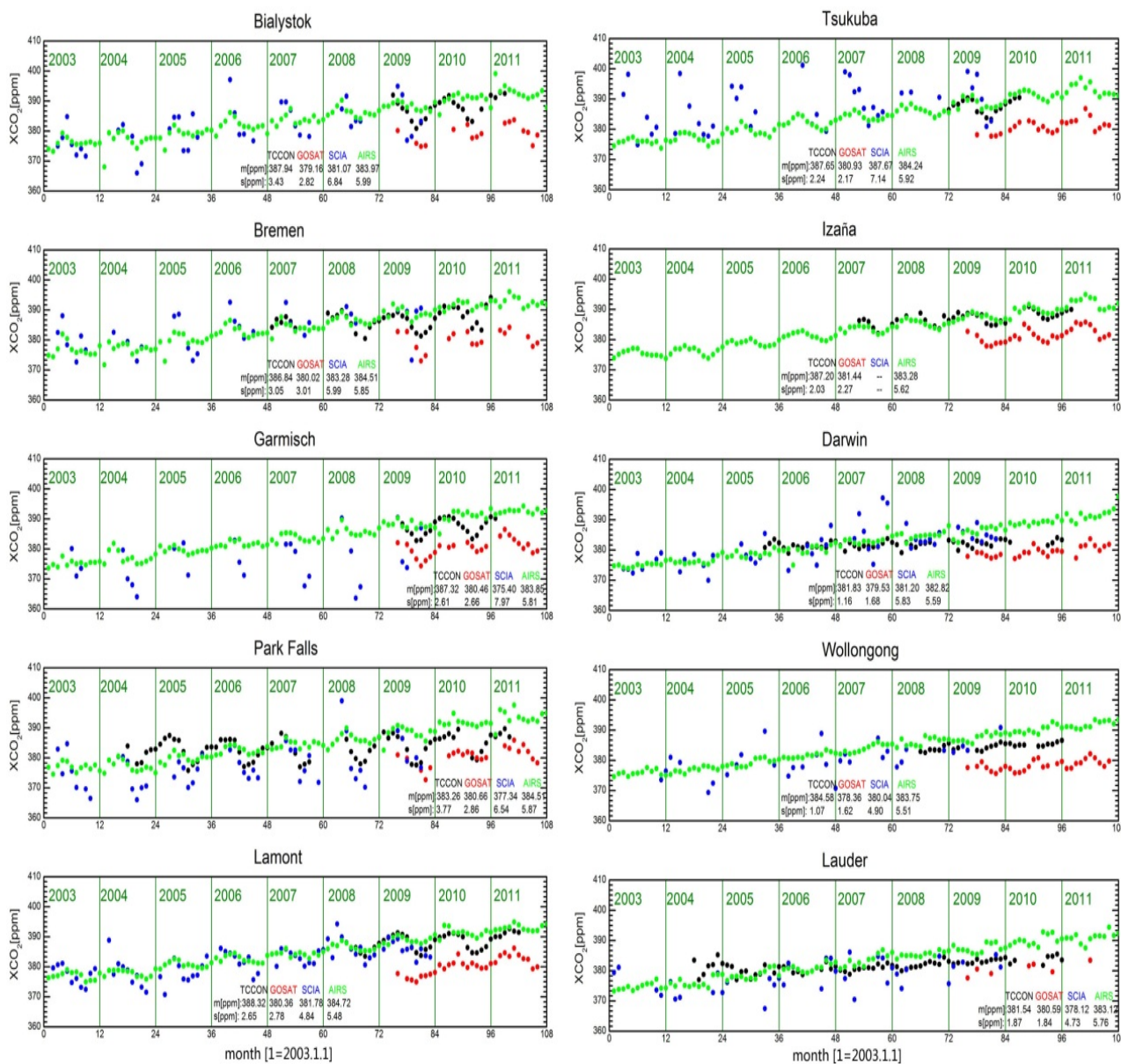
Table 3. Cont.

Location		GOSAT-FTS		SCIAMACHY-FTS		AIRS-FTS		
		09–11	03–08	09–11	03–11	03–08	09–11	03–11
Lamont (36.60°N, 97.49°W)	<i>n</i>	26	5	11	16	6	30	36
	<i>d</i> [ppm]	−8.43	−1.61	−2.06	−1.92	0.10	1.94	1.63
	<i>s</i> [ppm]	2.46	1.81	2.07	2.00	0.91	2.14	2.11
	<i>d</i> (100%)	−2.16	−0.41	−0.52	−0.49	0.02	0.50	0.42
	<i>s</i> (100%)	0.62	0.47	0.53	0.51	0.23	0.55	0.54
	<i>r</i>	0.61	0.38	0.66	0.69	0.88	0.58	0.69
Tsukuba (36.05°N, 140.12°E)	<i>n</i>	7	0	6	6	1	15	16
	<i>d</i> [ppm]	−8.14	-	4.30	4.30	−0.87	1.43	1.29
	<i>s</i> [ppm]	1.22	-	5.16	5.16	-	1.42	1.49
	<i>d</i> (100%)	−2.09	-	1.11	1.11	−0.22	0.37	0.33
	<i>s</i> (100%)	0.30	-	1.33	1.33	-	0.37	0.38
	<i>r</i>	0.91	-	0.79	0.79	-	0.79	0.77
Izaña (28.31°N, 16.5°W)	<i>n</i>	20	0	0	0	14	24	38
	<i>d</i> [ppm]	−7.19	-	-	-	−1.42	0.73	−0.05
	<i>s</i> [ppm]	0.89	-	-	-	0.86	1.29	1.55
	<i>d</i> (100%)	−1.85	-	-	-	−0.36	0.18	−0.01
	<i>s</i> (100%)	0.23	-	-	-	0.22	0.33	0.40
	<i>r</i>	0.90	-	-	-	0.89	0.74	0.81
Darwin (12.42°S, 130.89°E)	<i>n</i>	11	22	8	30	37	17	54
	<i>d</i> [ppm]	−3.99	2.14	3.34	2.46	0.59	4.78	1.91
	<i>s</i> [ppm]	0.83	5.36	2.41	4.79	2.53	1.93	3.06
	<i>d</i> (100%)	−1.04	0.56	0.87	0.64	0.15	1.25	0.50
	<i>s</i> (100%)	0.21	1.40	0.63	1.25	0.66	0.50	0.80
	<i>r</i>	0.56	0.60	−0.06	0.49	0.27	0.47	0.45
Wollongong (34.41°S, 150.88°E)	<i>n</i>	16	1	2	3	7	19	26
	<i>d</i> [ppm]	−7.28	−1.57	1.94	0.77	3.14	4.36	4.03
	<i>s</i> [ppm]	1.74	-	2.86	2.86	1.40	1.31	1.44
	<i>d</i> (100%)	−1.89	0.40	0.50	0.19	0.82	1.13	1.04
	<i>s</i> (100%)	0.45	-	0.74	0.74	0.36	0.34	0.37
	<i>r</i>	−0.04	-	1	0.89	0.06	0.59	0.61
Lauder (45.04°S, 169.68°E)	<i>n</i>	4	28	3	31	54	18	72
	<i>d</i> [ppm]	−4.43	−3.08	−0.70	−2.85	0.56	5.36	1.76
	<i>s</i> [ppm]	0.68	4.87	1.65	4.71	3.14	2.17	3.59
	<i>d</i> (100%)	−1.15	−0.80	−0.18	−0.74	0.14	1.39	0.46
	<i>s</i> (100%)	0.17	1.27	0.43	1.23	0.82	0.56	0.93
	<i>r</i>	0.77	−0.04	0.46	0.09	0.40	0.29	0.63

Table 4. Summary of Table 3.

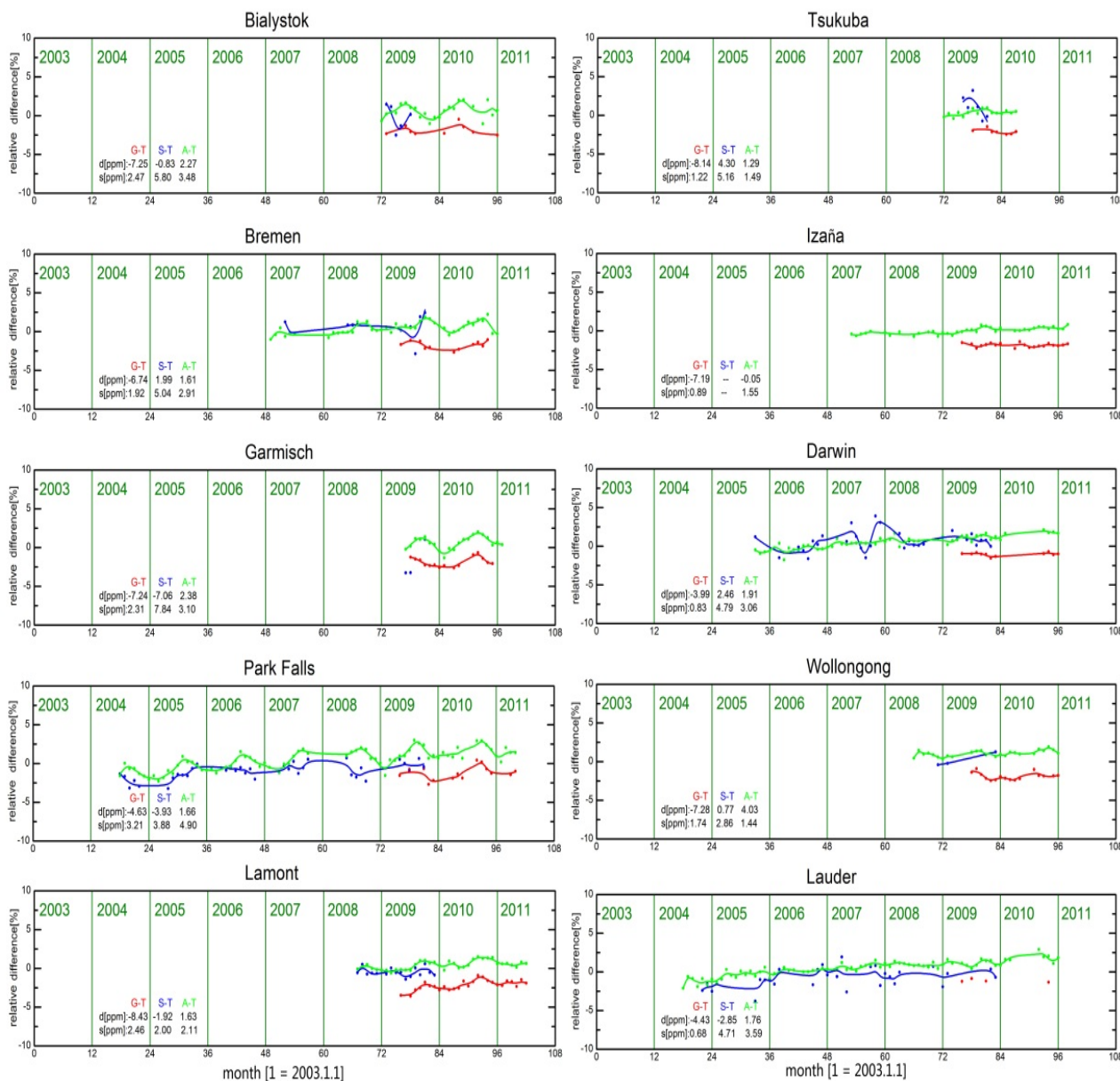
	GOSAT-FTS		SCIAMACHY-FTS		AIRS-FTS		
Time Period	09–11	03–08	09–08	03–11	03–08	09–08	03–11
Global Offset [ppm]	−6.53	−1.07	0.04	−0.78	0.21	2.81	1.84
Relative Precision [ppm]	1.77 (0.46%)	3.58	4.13	4.67 (1.22%)	2.19	2.56	2.76 (0.72%)
Relative Accuracy [ppm]	1.50 (0.38%)	2.51	3.19	3.35 (0.87%)	1.27	1.97	0.96 (0.25%)
Mean Correlation	0.64	0.49	0.41	0.43	0.46	0.51	0.56

Figure 3. Comparison of the GOSAT (red), SCIAMACHY (blue) and AIRS (green) XCO₂ time series of monthly means with g-b FTS measurements (black) at selected TCCON sites for the years 2003–2011. The following numbers have been computed based on the monthly averages: *m* is the mean vmr (in ppm) and *s* denotes the standard deviation of the monthly averages (in ppm).



Another more important error estimate is the relative accuracy: the relative accuracy of GOSAT data amounts to 1.50 ppm (0.38%) relative to g-b FTS data, that of SCIAMACHY is 3.35 ppm (0.87%) and that of AIRS is 0.96 ppm (0.25%) for the entire analyzed time period. Overall, we find a good agreement between the AIRS data and the reference data, and the GOSAT data present a good agreement with the g-b FTS data in the subperiod from 2009 to 2011.

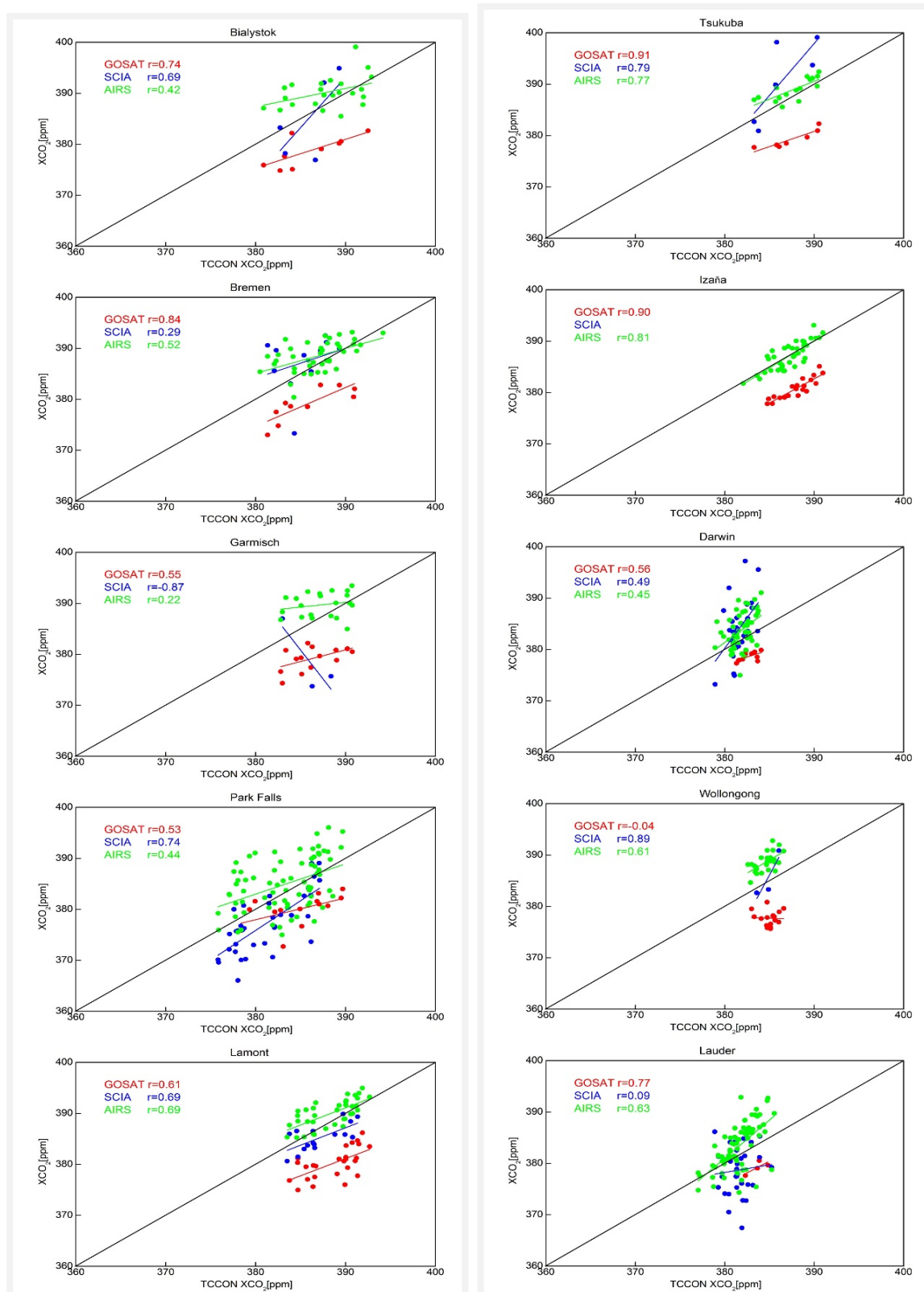
Figure 4. Percent differences between g-b FTS and the satellite products, GOSAT (red), SCIAMACHY (blue) and AIRS (green), at selected TCCON sites for the years 2003–2011. The solid lines have been smoothed using a five-month Hann window. The following numbers have been computed based on the monthly averages: *n* is the number of comparison pairs; *d* is the absolute mean difference (in ppm); and *s* denotes the standard deviation of the difference (in ppm). The complete results are summarized in Table 2.



Scatter diagrams of the time series of the satellite products and g-b FTS data for XCO₂ with the correlation coefficients at selected TCCON sites are shown in Figure 5. We only plotted data for which the g-b FTS data were averaged for a month and the corresponding satellite XCO₂ values were successfully retrieved. Therefore, there are fewer satellite data points in the scatter diagrams than are listed in the time series. The g-b FTS data at Darwin were not obtained between February, 2010, and August, 2010, due to mechanical problems with the sun tracker. Only a few GOSAT and SCIAMACHY data are available for comparison with Bialystok, Bremen, Garmisch, Tsukuba and Lauder, and no SCIAMACHY data are available at the Izaña site. SCIAMACHY data have an

opposing trend from the g-b FTS data at Garmisch, mainly because of fewer available data. Due to using the monthly mean data, the mean correlation coefficients of the three satellite data are less than 0.5.

Figure 5. Scatter diagrams of the time series of the satellite product, GOSAT (red), SCIAMACHY (blue) and AIRS (green) and g-b FTS data, for XCO₂ at selected TCCON sites and the correlation coefficient (*r*). The solid lines are the trend for each satellite product.



4.2. Seasonal Accuracy

To obtain the seasonal accuracy of all types of satellite products, we performed a seasonal comparison for them. The comparison methodology is similar to Section 3.2, but the time interval is different. The entire analyzed time period can be divided into four subperiods according to four seasons. The results of seasonal comparisons for each site are shown in Table 5. Table 6 summarizes the results.

Table 5. Validation and comparison results for three XCO₂ satellite products based on monthly data in four seasons from 2003 to 2011. The characters, G, S, A, and F, stand for GOSAT, SCIAMACHY, AIRS and g-b FTS, respectively.

Location		Spring			Summer			Autumn			Winter		
		G-F	S-F	A-F	G-F	S-F	A-F	G-F	S-F	A-F	G-F	S-F	A-F
Bialystok	<i>n</i>	3	2	7	3	2	6	3	1	4	0	0	6
	<i>d</i> [ppm]	−9.29	5.04	1.19	−4.10	−7.39	5.37	−8.35	0.54	2.84	-	-	0.05
	<i>s</i> [ppm]	0.39	0.57	2.17	1.62	2.31	2.32	0.46	-	2.17	-	-	4.05
	<i>d</i> (100%)	−2.37	1.29	0.30	−1.07	−1.91	1.40	−2.17	0.14	0.74	-	-	0.01
	<i>s</i> (100%)	0.09	0.14	0.55	0.42	0.59	0.60	0.11	-	0.56	-	-	1.03
Bremen	<i>n</i>	3	4	12	4	6	9	4	1	9	0	0	11
	<i>d</i> [ppm]	−8.62	1.99	0.63	−5.24	0.77	2.95	−6.82	9.24	4.09	-	-	−0.44
	<i>s</i> [ppm]	1.60	2.14	1.77	0.80	5.77	2.37	1.64	-	3.04	-	-	2.04
	<i>d</i> (100%)	−2.21	0.51	0.16	−1.35	0.20	0.76	−1.78	2.42	1.06	-	-	−0.11
	<i>s</i> (100%)	0.41	0.55	0.45	0.20	1.50	0.61	0.43	-	0.79	-	-	0.52
Garmisch	<i>n</i>	3	4	12	5	1	6	6	1	6	2	0	5
	<i>d</i> [ppm]	−8.62	1.99	0.63	−4.57	−12.54	4.62	−7.88	4.02	3.57	−9.63	-	−0.68
	<i>s</i> [ppm]	1.60	2.14	1.77	1.33	-	2.18	1.21	-	2.01	0.53	-	2.76
	<i>d</i> (100%)	−2.20	0.515	0.16	−1.18	−3.24	1.208	−2.04	1.051	0.92	−2.47	-	−0.17
	<i>s</i> (100%)	0.40	0.55	0.45	0.34	-	0.56	0.31	-	0.52	0.13	-	0.70
Park Falls	<i>n</i>	6	9	18	2	17	19	6	9	19	0	0	17
	<i>d</i> [ppm]	−5.91	−2.70	0.62	−0.64	−4.27	4.22	−4.68	−4.52	2.32	-	-	−0.84
	<i>s</i> [ppm]	1.20	4.45	4.08	2.28	3.13	4.49	3.73	4.285	4.74	-	-	4.73
	<i>d</i> (100%)	−1.52	−0.70	0.16	−0.16	−1.12	1.11	−1.22	−1.19	0.61	-	-	−0.22
	<i>s</i> (100%)	0.30	1.15	1.05	0.59	0.82	1.18	0.97	1.12	1.24	-	-	1.22
Lamont	<i>n</i>	7	3	9	7	5	9	6	6	9	6	2	9
	<i>d</i> [ppm]	−8.84	−3.19	0.70	−8.71	−1.47	2.15	−7.01	−1.83	2.89	−9.04	−1.38	0.79
	<i>s</i> [ppm]	2.58	1.59	1.34	3.05	2.23	2.12	1.58	1.85	2.07	1.57	1.55	1.93
	<i>d</i> (100%)	−2.25	−0.81	0.18	−2.24	−0.38	0.55	−1.81	−0.47	0.75	−2.31	−0.35	0.20
	<i>s</i> (100%)	0.65	0.40	0.34	0.78	0.57	0.55	0.40	0.48	0.53	0.40	0.39	0.49
Tsukuba	<i>n</i>	1	2	4	1	3	3	3	1	3	2	0	6
	<i>d</i> [ppm]	−8.22	6.33	0.99	−7.62	4.57	2.69	−7.40	−0.58	2.01	−9.46	-	0.42
	<i>s</i> [ppm]	-	2.42	1.01	-	6.21	1.25	1.29		1.18	0.05	-	1.30
	<i>d</i> (100%)	−2.10	1.62	0.25	−1.97	1.18	0.69	−1.91	−0.15	0.52	−2.42	-	0.10
	<i>s</i> (100%)	-	0.62	0.26	-	1.61	0.32	0.33	-	0.31	0.01	-	0.33

Table 5. Cont.

Location		Spring			Summer			Autumn			Winter		
		G-F	S-F	A-F	G-F	S-F	A-F	G-F	S-F	A-F	G-F	S-F	A-F
Izaña	<i>n</i>	4	0	8	6	0	11	6	0	10	4	0	9
	<i>d</i> [ppm]	-6.88	-	-0.29	-7.87	-	-0.28	-6.92	-	0.46	-6.90	-	-0.15
	<i>s</i> [ppm]	1.31	-	0.68	0.67	-	1.72	0.52	-	1.53	0.48	-	1.75
	<i>d</i> (100%)	-1.76	-	-0.07	6	0	11	-1.79	-	0.12	-1.77	-	-0.03
	<i>s</i> (100%)	0.33	-	0.17	-2.02	-	-0.07	0.13	-	0.39	0.12	-	0.45
Darwin	<i>n</i>	1	7	12	3	12	12	6	9	15	1	2	15
	<i>d</i> [ppm]	-3.67	4.06	1.04	-3.64	0.07	1.86	-4.25	4.74	2.09	-3.81	1.00	2.47
	<i>s</i> [ppm]		3.61	3.13	0.30	3.49	2.05	1.04	4.96	3.78		6.69	2.69
	<i>d</i> (100%)	-0.96	1.06	0.27	-0.95	0.01	0.48	-1.11	1.24	0.54	-0.99	0.26	0.64
	<i>s</i> (100%)		0.95	0.82	0.07	0.91	0.53	0.26	1.29	0.99	-	1.76	0.70
Wollongong	<i>n</i>	2	0	2	5	0	8	5	2	9	4	1	7
	<i>d</i> [ppm]	-8.83	-	4.06	-5.19	-	4.55	-8.24	1.61	4.28	-7.92	-0.91	3.11
	<i>s</i> [ppm]	0.30	-	0.33	1.35	-	1.30	0.94	3.19	1.61	0.750	-	1.06
	<i>d</i> (100%)	-2.2	-	1.05	-1.35	-	1.18	-2.13	0.41	1.11	-2.05	-0.23	0.80
	<i>s</i> (100%)	0.07	-	0.08	0.35	-	0.34	0.24	0.82	0.41	0.19	-	0.27
Lauder	<i>n</i>	1	4	14	1	0	18	2	14	21	0	13	19
	<i>d</i> [ppm]	-4.68	-0.21	1.96	-3.31	-	1.32	-4.87	-2.77	1.92	-	-3.74	1.85
	<i>s</i> [ppm]	-	6.23	2.15	-	-	3.91	0.29	5.23	3.97	-	2.93	3.644
	<i>d</i> (100%)	-1.22	-0.05	0.51	-0.86	-	0.34	-1.26	-0.72	0.50	-0.98	0.48	-0.98
	<i>s</i> (100%)	-	1.64	0.56	-	-	1.02	0.07	1.37	1.03	0.769	0.95	0.76

Table 6. Summary of Table 5.

	Spring			Summer			Autumn			Winter		
	G-F	S-F	A-F									
Global Offset[ppm]	-7.35	1.66	1.15	-5.08	-2.89	2.94	-6.64	1.16	2.64	-7.79	-1.25	0.65
Relative	1.28	2.89	1.84	1.43	3.86	2.37	1.27	3.90	2.61	0.67	3.72	2.6
Precision[ppm]	(0.32%)	(0.75%)	(0.47%)	(0.09%)	(1.00%)	(0.60%)	(0.33%)	(1.01%)	(0.68%)	(0.27%)	(1.03%)	(0.65%)
Relative	1.87	3.26	1.11	2.31	5.27	1.66	1.43	4.03	1.08	2.01	1.68	1.30
Accuracy[ppm]	(0.46%)	(0.84%)	(0.30%)	(2.23%)	(1.30%)	(3.10%)	(0.36%)	(1.06%)	(0.28%)	(0.59%)	(0.34%)	(0.46%)

The error estimate for each satellite product in the four seasons is the relative accuracy listed in Table 6. In spring, the global offset and relative accuracy of AIRS data are as low as 1.15 ppm and 1.11 ppm (0.30%), respectively. In summer, the relative precision and accuracy of GOSAT data are 1.43 ppm (0.09%) and 2.31 ppm (2.23%), respectively. In autumn, the global offset of SCIAMACHY data is only 1.16 ppm, but the regional bias is a little higher at 4.03 ppm (1.06%). In winter, the comparative data sets are fewer, except for AIRS, which has global offset and regional biases of 0.65 ppm and 1.30 ppm (0.46%), respectively. Because the AIRS data are averaged within a larger scope, the fluctuation range is relatively smaller than 1.3 ppm.

4.3. Annual Increase and Seasonal Cycle

We calculated the linear trends of the year separately in cases where data for the year are available for a sufficient number (more than three years of data). First, we calculate the increment of the *i*th month in a year as follows:

$$m_i^y = x_i^y - x_i^{y-1}, (i = 1,2,3, \dots, 12; y = 2004, \dots, 2011) \tag{3}$$

Therefore, we can obtain up to 12 individual trends (e.g., one for all Januarys). We can then calculate the linear trend of each site, $\{m_i^{2004}, m_i^{2005}, \dots, m_i^{2011} (i = 1, 2, 3, \dots, 12)\}$, and the annual increase is the mean of the trend, $Inc = \frac{\sum_{y=2004}^{2011} \sum_{i=1}^{12} m_i^y}{n}$, where n is the number of increments. The annual increases listed in Table 7 are derived by fitting a linear trend to the deseasonalized time series. The mean amplitude of the seasonal cycle is obtained by subtracting the linear trend derived above from the time series. Then, we average the resulting amplitudes for all years in which the cycle is reasonably sampled, denoting the standard error of the mean as an error. The average peak-to-peak amplitude of the seasonal cycles is also listed in Table 7; *std* is the standard deviation of the increments. Time series of the XCO₂ yearly linear increasing trends are shown in Figure 6.

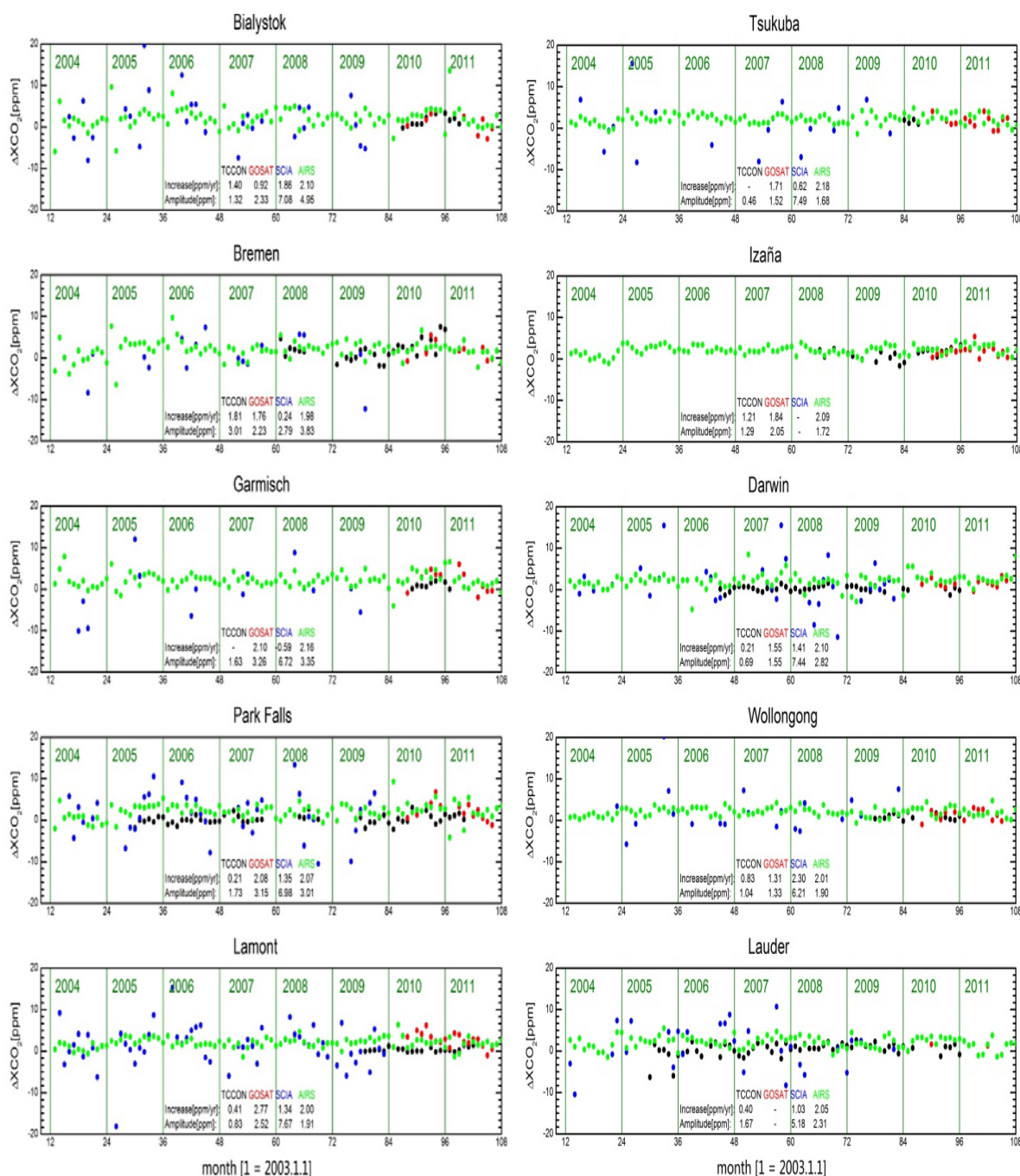
Table 7. Annual increase and seasonal cycle amplitude at the analyzed TCCON sites.

Location		Annual Increase [ppm per year]				Seasonal Cycle Amplitude [ppm]			
		TCCON	GOSAT	SCIA	AIRS	TCCON	GOSAT	SCIA	AIRS
	<i>n</i>	23	16	40	108	2	2	6	8
Bialystok	<i>value</i>	1.40	0.92	1.86	2.10	1.32	2.33	7.08	4.95
	<i>std</i>	1.14	2.22	5.91	2.53	0.62	0.71	5.63	3.02
	<i>n</i>	41	17	33	108	3	2	6	8
Bremen	<i>value</i>	1.81	1.76	0.24	1.98	3.01	2.23	2.79	3.83
	<i>std</i>	2.23	2.07	4.81	2.24	2.15	1.53	2.67	1.98
	<i>n</i>	21	25	27	108	1	2	4	8
Garmisch	<i>value</i>	-	2.10	-0.59	2.16	1.63	3.26	6.72	3.35
	<i>std</i>	-	2.47	6.06	1.74	-	0.60	4.56	1.30
	<i>n</i>	73	22	46	108	6	2	6	8
Park Falls	<i>value</i>	0.21	2.08	1.35	2.07	1.73	3.15	6.98	3.01
	<i>std</i>	1.05	2.06	5.34	1.9	0.78	1.55	2.95	1.72
	<i>n</i>	36	30	72	108	3	2	6	8
Lamont	<i>value</i>	0.41	2.77	1.34	2.00	0.83	2.52	7.67	1.91
	<i>std</i>	0.51	1.68	4.79	1.21	0.19	0.94	3.09	1.16
	<i>n</i>	16	24	41	107	2	2	5	8
Tsukuba	<i>value</i>	-	1.71	0.62	2.18	0.46	1.52	7.49	1.68
	<i>std</i>	-	1.4	6.0	1.19	0.06	0.86	3.82	0.63
	<i>n</i>	38	30	0	108	3	2	-	8
Izaña	<i>value</i>	1.21	1.84	-	2.09	1.29	2.05	-	1.72
	<i>std</i>	1.22	1.19	-	1.10	0.66	1.49	-	0.28
	<i>n</i>	54	26	50	108	5	2	6	8
Darwin	<i>value</i>	0.21	1.55	1.41	2.10	0.69	1.55	7.44	2.82
	<i>std</i>	0.62	0.92	5.44	1.79	0.55	0.23	4.95	2.03
	<i>n</i>	26	29	34	108	2	2	5	8
Wollongong	<i>value</i>	0.83	1.31	2.30	2.01	1.04	1.33	6.21	1.90
	<i>std</i>	0.61	1.13	5.37	1.06	0.16	0.35	6.09	0.56

Table 7. Cont.

Location	Annual Increase [ppm per year]				Seasonal Cycle Amplitude [ppm]			
	TCCON	GOSAT	SCIA	AIRS	TCCON	GOSAT	SCIA	AIRS
<i>n</i>	72	7	39	108	6	2	6	8
Lauder <i>value</i>	0.40	-	1.03	2.05	1.67	-	5.18	2.31
<i>std</i>	1.64	-	5.23	1.47	0.37	-	3.51	0.57
Mean value	0.81	1.78	1.06	2.07	1.37	2.21	6.39	2.75
<i>std</i>	1.12	1.68	5.43	1.62	0.61	0.92	4.14	1.32

Figure 6. Time series of XCO₂ year-to-year linear increasing trends of the satellite product, GOSAT (red), SCIAMACHY (blue), AIRS (green) and g-b FTS (black), at selected TCCON sites.



According to Table 7, there are generally no significant differences between satellite data and the annual increase according to g-b FTS data. The Lauder site has a seasonal cycle in XCO₂ with a small peak-to-peak amplitude of approximately 0.6 ppm. The measurements over Wollongong reach approximately 2 ppm peak-to-peak. The Lauder XCO₂ time series is the longest in the Southern Hemisphere and has had a consistent increase of 1.89 ppm per year since 2004 [44]. For all sites, the increases agree within their errors, with the exception of Park Falls and Lamont, where a marginal residual difference remains after considering the standard errors for SCIAMACHY [22]. Nevertheless, the global mean increase is somewhat larger for satellite data than for g-b FTS data (1.78 ± 1.68 , 1.06 ± 5.43 and 2.07 ± 1.62 ppm per year compared to 0.81 ± 1.12 ppm per year). The highest annual increase among the three satellite products is measured by AIRS, at 2.07 ppm per year. However, the TCCON increase at Bremen is significantly larger than the one for the GOSAT and SCIAMACHY time series (1.81 ± 2.23 ppm per year compared to 1.76 ± 2.07 and 0.24 ± 4.81 ppm per year).

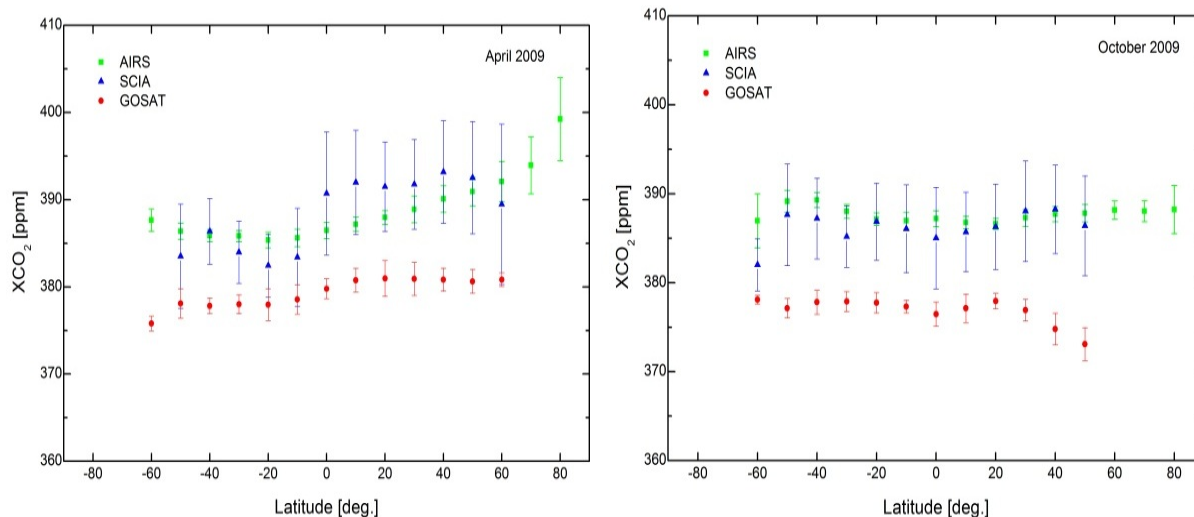
To obtain a quantitative impression of the global seasonal cycle differences and their significance, we calculate the mean amplitudes for all TCCON sites where estimated seasonal cycle amplitudes are available for all three data sets. After subtracting the linear trend, *i.e.*, the year-to-year increase, we calculate the average peak-to-peak amplitude of the seasonal cycles. The seasonal cycles in all data sets are in close agreement. The average peak to peak amplitudes are 1.37 ± 0.61 ppm for the g-b FTS, 2.21 ± 0.92 ppm for GOSAT, 6.39 ± 4.14 ppm for SCIAMACHY and 2.75 ± 1.32 ppm for AIRS. Due to SCIAMACHY's relatively large standard error, there are significant differences between SCIAMACHY and the other data sets. The amplitudes derived from SCIAMACHY are typically larger than those from other satellite data sets, which are, in turn, larger than those from TCCON.

4.4. Latitudinal Distribution of Zonal Averaged Satellite Data

To analyze the spatial consistency and regional differences between remote sensing data, the monthly means of zonal averaged satellite data are calculated for each 10° band of latitude. Latitudinal distributions of monthly means of zonal averaged satellite data of XCO₂ in April 2009, and in October, 2009, are shown in Figure 7. In summer and autumn, the strong photosynthesis by lush vegetation leads to the decrease of the CO₂ concentration until its minimum in October. In winter and spring, the weak photosynthesis of the withered vegetation and winter heating lead to higher CO₂ concentrations, which reach peak in April.

All data sets show that XCO₂ is higher in the Northern Hemisphere compared to the Southern Hemisphere in April, but the difference between the hemispheres is small in October. The GOSAT data are approximately 10 ppm lower in the northern mid-latitudes and nearly 15 ppm lower in the southern mid-latitudes than the other data sets.

Figure 7. Latitudinal distributions of monthly means of zonal averaged GOSAT (red), SCIAMACHY (blue) and AIRS (green) of XCO₂ for each 10° latitudinal band in April and October 2009. The vertical bars correspond to the standard deviations of the data within a given band.



5. Discussions

Column average dry air mole fractions of CO₂ from 2003 to 2011 have been compared using GOSAT (2009–2011), SCIAMACHY (2003–2009), AIRS (2003–2011) and g-b FTS measurements. The comparison is also performed for global zonal averages latitudinal from 60° S to 80° N in 10° steps. The comparison is performed by comparing monthly mean data in the entire analyzed time period and two subperiods, respectively. Both approaches yield similar results.

Among the three satellite products, the accuracy of SCIAMACHY data is relatively low, and the observation range is limited. The scatter of GOSAT retrievals is well below 1%, though this is a substantial improvement over earlier GOSAT validation efforts [4,28]. The XCO₂ data retrieved from SCIAMACHY perform better in inland areas. The values of SCIAMACHY are lower than g-b FTS, but the difference is never more than 2 ppm. The XCO₂ data retrieved from SCIAMACHY are inferior in offshore areas and the difference is larger. The XCO₂ data values retrieved from GOSAT are lower than g-b FTS and the difference amounts to 7 ppm. However, the GOSAT data do match well with g-b FTS on islands. This finding shows that the stability and correlation of GOSAT data have improved globally, especially in oceanic and offshore areas. The AIRS data products have the distinct advantage in terms of coverage range and measurement accuracy, which also provides more opportunity for comparisons with g-b FTS data. The absence of some high values in the AIRS data is consistent with the mid- and upper troposphere, being less sensitive to surface emissions [51]. We also sampled both SCIAMACHY and AIRS data sets within ±2.5 degrees and, then, compared with the original data. The results are listed in Table 8.

The differences of global offset and mean correlation are small. However, the different spatial resolution imperfect match has significantly contributed to the observed standard deviations [50].

We have also estimated linear trends from monthly mean data for different periods. In general, the XCO₂ seasonal cycle amplitudes derived from satellite data are somewhat larger than those from g-b

FTS data. Because the time periods considered at certain TCCON sites are rather short, these trend estimates are only used to identify potential instrumental issues with the GOSAT and SCIAMACHY data. Although the XCO₂ retrievals from AIRS are in the troposphere, the products are more consistent with the g-b FTS measurements.

Table 8. Comparison of SCIAMACHY and AIRS data sets within ± 2.5 degrees with the original data, where SCIA and AIRS are the original data; SCIA' and AIRS' are the sampled data within ± 2.5 degrees.

	SCIA-FTS	SCIA'-FTS	AIRS-FTS	AIRS'-FTS
Global Offset [ppm]	-0.78	-0.70	1.84	1.81
Relative Precision [ppm]	4.67(1.22%)	4.12(1.07%)	2.76(0.72%)	2.68(0.70%)
Relative Accuracy [ppm]	3.35(0.87%)	1.65(0.43%)	0.96(0.25%)	1.01(0.26%)
Mean Correlation	0.43	0.45	0.56	0.57

The relative accuracy of AIRS data is 1.11 ppm (0.30%) and 1.08 ppm (0.28%) in spring and autumn, respectively. The relative accuracy of GOSAT data is 2.31 ppm (2.23%) in summer and SCIAMACHY data is 1.68 ppm (0.34%) in winter. Although there are different biases for XCO₂, the satellite data retrievals and g-b FTS data show similar seasonal behaviors over the Northern Hemisphere: higher in spring and lower in autumn. The seasonal change in atmospheric CO₂ concentration is mainly influenced by CO₂ absorption and emission by terrestrial ecosystems. In summer and autumn, the strong photosynthesis of the lush vegetation leads to the decrease of the CO₂ concentration and reaches to a low in October. In winter and spring, weak photosynthesis and winter heating lead to higher CO₂ concentrations, which maintain a higher level and peak in April.

6. Conclusions

In this paper, we analyze the XCO₂ products retrieved from Imaging Absorption Spectrometer for Atmospheric Cartography (SCIAMACHY), Greenhouse Gases Observing Satellite (GOSAT), Atmospheric Infrared Sounder (AIRS) and use high-resolution ground-based Fourier Transform Spectrometers (g-b FTS) with reference to calibration data obtained at ten Total Carbon Column Observing Network (TCCON) from 2003 to 2011. The validation and comparison reveal that the satellite data are biased by -6.53 ± 1.77 ppm (0.46%), -0.78 ± 4.67 ppm (1.22%) and 1.84 ± 2.76 ppm (0.72%) for GOSAT, SCIAMACHY and AIRS relative to the reference values, respectively. The relative accuracy of these satellite data are 1.50 ppm (0.38%), 3.35 ppm (0.87%) and 0.96 ppm (0.25%), respectively, and the mean correlation coefficients are 0.64, 0.43 and 0.56 compared to g-b FTS data, respectively. The mean annual increase in XCO₂ of GOSAT, SCIAMACHY, AIRS and g-b FTS data are 1.78, 1.06, 2.07 and 0.81 ppm per year, respectively. The relative accuracy of AIRS data is 1.11 ppm (0.30%) and 1.08 ppm (0.28%) in spring and autumn, respectively. The relative accuracy of GOSAT data is 2.31 ppm (2.23%) in summer and SCIAMACHY data, 1.68 ppm (0.34%) in winter. Due to the product selection for validation, the spatial distributions in XCO₂ between three sensor measurements are different. The SCIAMACHY data are confined to the land, because of lower surface reflectance; GOSAT XCO₂ data are filtered for aerosol optical depth less than 0.5 and are removed

over high mountain ranges. AIRS XCO₂ product get larger global data coverage scale by losing accuracy in the product process.

GOSAT data offer certain advantages, but also have high systemic bias. The XCO₂ data retrieved from SCIAMACHY perform better in inland areas, but the difference is larger. Compared to the differences between the former two satellites, the system bias of AIRS is lowest for each site. Especially in mid-latitude regions, the AIRS XCO₂ values agree very well with g-b FTS. Overall, AIRS data show largely the same trend as the g-b FTS data. Therefore, the AIRS data product can reflect the distribution characteristics and change rules for global CO₂ atmospheric concentration very well. The uncertainties in sensor measurements are about the cloud, lower surface reflectance and systematic deviations, due to aerosols, thin cirrus clouds and even spectrum instrument depreciation of sensor. The accuracies of satellite data is also affected by the accuracies of retrieval algorithm. In the future, we plan to investigate interferences by aerosols and thin cirrus clouds using aerosol LIDaRs and/or sky-radiometers at selected FTS sites. Further improvements could be achieved by evaluating systematic errors with an empirical neural-network-type multivariate regression with physically meaningful regression coefficients in an approach similar to [52] or by accounting for additional physical parameters in future models (e.g., cloud parameters, as in [34,53]).

Acknowledgments

We thank the members of the GOSAT Project (JAXA, NIES and Ministry of the Environment, Japan) for providing GOSAT Level 2 data products. We thank the University of Bremen for providing us with the SCIAMACHY Level 2 data products. We thank NASA Goddard Earth Science Data and Information Services Center for providing us with the AIRS Version 5 Level 3 CO₂ data products. We also thank NASA's Terrestrial Ecology Program and the Orbiting Carbon Observatory for their support of TCCON.

This study was supported by the Public Welfare Special Program, Ministry of Environmental Protection of the People's Republic of China (grant 200909018), the National Natural Science Foundation of China (No. 41001215), the Youth Science Funds of LREIS, CAS., and the Gray Haze Remote Sensing Monitoring Technology Research and Operation Demonstration of JiangSu Province (Grant No. 201130).

Conflict of Interest

The authors declare no conflict of interest.

References and Notes

1. Intergovernmental Panel on Climate Change (IPCC). *Climate Change 2007: The Physical Science Basis: Contribution of Working Group I to the Fourth Assessment Report of the Intergovernmental Panel on Climate Change*; Solomon, S., Qin, D., Manning, M., Chen, Z., Marquis, M., Averyt, K.B., Tignor, M., Miller, H.L., Eds.; Cambridge University Press: Cambridge, UK and New York, NY, USA, 2007; p. 996.

2. Cox, P.M.; Betts, R.A.; Jones, C.D.; Spall, S.A.; Totterdell, I.J. Acceleration of global warming due to carbon-cycle feedbacks in a coupled climate model. *Nature* **2000**, *408*, 184–187.
3. Bousquet, P.; Peylin, P.; Ciais, P.; Le Quéré, C.; Friedlingstein, P.; Tans, P.P. Regional changes in carbon dioxide fluxes of land and oceans since 1980. *Science* **2000**, *290*, 1342–1346.
4. Morino, I.; Uchino, O.; Inoue, M.; Yoshida, Y.; Yokota, T.; Wennberg, P.O.; Rettinger, M. Preliminary validation of column-averaged volume mixing ratios of carbon dioxide and methane retrieved from GOSAT short-wavelength infrared spectra. *Atmos. Meas. Tech.* **2011**, *4*, 1061–1076.
5. Butz, A.; Guerlet, S.; Hasekamp, O.; Schepers, D.; Galli, A.; Aben, I.; Warneke, T. Toward accurate CO₂ and CH₄ observations from GOSAT. *Geophys. Res. Lett.* **2011**, *38*, L14812.
6. Parker, R.; Boesch, H.; Cogan, A.; Fraser, A.; Feng, L.; Palmer, P. I.; Wunch, D. Methane observations from the Greenhouse Gases Observing SATellite: Comparison to ground-based TCCON data and model calculations. *Geophys. Res. Lett.* **2011**, *38*, L15807.
7. Burrows, J.P.; Hölzle, E.; Goede, A.P.H.; Visser, H.; Fricke, W. SCIAMACHY-Scanning imaging absorption spectrometer for atmospheric cartography. *Acta Astronaut.* **1995**, *35*, 445–451.
8. Bovensmann, H.; Burrows, J.P.; Buchwitz, M.; Frerick, J.; Noël, S.; Rozanov, V.V.; Goede, A.P.H. SCIAMACHY: Mission objectives and measurement modes. *J. Atmos. Sci.* **1999**, *56*, 127–150.
9. Yokota, T.; Yoshida, Y.; Eguchi, N.; Ota, Y.; Tanaka, T.; Watanabe, H.; Maksyutov, S. Global concentrations of CO₂ and CH₄ retrieved from GOSAT: First preliminary results. *Sola.* **2009**, *5*, 160–163.
10. Aumann, H.H.; Chahine, M.T.; Gautier, C.; Goldberg, M.D.; Kalnay, E.; McMillin, L.M.; Susskind, J. AIRS/AMSU/HSB on the Aqua mission: Design, science objectives, data products, and processing systems. *IEEE Trans. Geosci. Remote Sens.* **2003**, *41*, 253–264.
11. Crisp, D.; Atlas, R.M.; Breon, F.M.; Brown, L.R.; Burrows, J.P.; Ciais, P.; Schroll, S. The orbiting carbon observatory (OCO) mission. *Adv. Space. Res.* **2004**, *34*, 700–709.
12. Boesch, H.; Baker, D.; Connor, B.; Crisp, D.; Miller, C. Global characterization of CO₂ column retrievals from shortwave-infrared satellite observations of the Orbiting Carbon Observatory-2 mission. *Remote Sens.* **2011**, *3*, 270–304.
13. Bovensmann, H.; Buchwitz, M.; Burrows, J. P.; Reuter, M.; Krings, T.; Gerilowski, K.; Erzinger, J. A remote sensing technique for global monitoring of power plant CO₂ emissions from space and related applications. *Atmos. Meas. Tech.* **2010**, *3*, 781–811.
14. Krings, T.; Gerilowski, K.; Buchwitz, M.; Reuter, M.; Tretner, A.; Erzinger, J.; Bovensmann, H. MAMAP—A new spectrometer system for column-averaged methane and carbon dioxide observations from aircraft: retrieval algorithm and first inversions for point source emission rates. *Atmos. Meas. Tech.* **2011**, *4*, 1735–1758.
15. Velasco, V.; Buchwitz, M.; Bovensmann, H.; Reuter, M.; Schneising, O.; Heymann, J.P.; Burrows, J.P. Towards space based verification of CO₂ emissions from strong localized sources: fossil fuel power plant emissions as seen by a CarbonSat constellation. *Atmos. Meas. Tech.* **2011**, *4*, 2809–2822.
16. Liu, Y.; Yin, Z.; Yang, Z.; Zheng, Y.; Yan, C.; Yang, D. Chinese Carbon Dioxide Observation Satellite (TanSat) Project. In Proceedings of AGU Fall Meeting, San Francisco, CA, USA, 3–7 December 2011; Abstract #A42D-02.
17. Liu, Y.; Yang, D.; Cai, Z. A retrieval algorithm for TanSat XCO₂ observation: Retrieval experiments using GOSAT data. *Chinese Sci. Bull.* **2013**, *58*, 1–4.

18. Cogan, A.J.; Boesch, H.; Parker, R.J.; Feng, L.; Palmer, P.I.; Blavier, J.F.; Wunch, D. Atmospheric carbon dioxide retrieved from the Greenhouse gases Observing SATellite (GOSAT): Comparison with ground-based TCCON observations and GEOS-Chem model calculations. *J. Geophys. Res.* **2012**, *117*, D21301, doi:10.1029/2012JD018087, 1–17.
19. Yoshida, Y.; Kikuchi, N.; Morino, I.; Uchino, O.; Oshchepkov, S.; Bril, A.; Yokota, T. Improvement of the retrieval algorithm for GOSAT SWIR XCO₂ and XCH₄ and their validation using TCCON data. *Atmos. Meas. Tech.* **2013**, *6*, 949–988.
20. Inoue, M.; Morino, I.; Uchino, O.; Miyamoto, Y.; Yoshida, Y.; Yokota, T.; Patra, P.K. Validation of XCO₂ derived from SWIR spectra of GOSAT TANSO-FTS with aircraft measurement data. *Atmos. Chem. Phys. Discuss.* **2013**, *13*, 3203–3246.
21. Schneising, O.; Buchwitz, M.; Reuter, M.; Heymann, J.; Bovensmann, H.; Burrows, J.P. Long-term analysis of carbon dioxide and methane column-averaged mole fractions retrieved from SCIAMACHY. *Atmos. Chem. Phys.* **2011**, *11*, 2863–2880.
22. Schneising, O.; Bovensmann, H.; Buchwitz, M.; Burrows, J.P.; Deutscher, N.M.; Griffith, D.W.; Wunch, D. Atmospheric greenhouse gases retrieved from SCIAMACHY: Comparison to ground-based FTS measurements and model results. *Atmos. Chem. Phys.* **2012**, *12*, 1527–1540.
23. Wang, K.; Jiang, H.; Zhang, X.; Zhou, G. Analysis of spatial and temporal variations of carbon dioxide over China using SCIAMACHY satellite observations during 2003–2005. *Int. J. Remote Sens.* **2011**, *32*, 815–832.
24. Bai, W.; Zhang, X.; Zhang, P. Temporal and spatial distribution of tropospheric CO₂ over China based on satellite observations. *Chinese Sci. Bull.* **2010**, *55*, 3612–3618.
25. Kuze, A.; Suto, H.; Nakajima, M.; Hamazaki, T. Thermal and near infrared sensor for carbon observation Fourier-transform spectrometer on the Greenhouse Gases Observing Satellite for greenhouse gases monitoring. *Appl. Opt.* **2009**, *48*, 6716–6733.
26. Hamazaki, T.; Kaneko, Y.; Kuze, A.; Kondo, K. Fourier transform spectrometer for Greenhouse Gases Observing Satellite (GOSAT). *Proc. SPIE* **2004**, *5659*, 73–80.
27. Rodgers, C.D. Optimal Linear Inverse Methods. In *Inverse Methods for Atmospheric Sounding: Theory and Practice*; World Scientific: Singapore, 2000; pp. 65–79.
28. Yoshida, Y.; Ota, Y.; Eguchi, N.; Kikuchi, N.; Nobuta, K.; Tran, H.; Yokota, T. Retrieval algorithm for CO₂ and CH₄ column abundances from short-wavelength infrared spectral observations by the Greenhouse Gases Observing Satellite. *Atmos. Meas. Tech.* **2011**, *4*, 717–734.
29. Burrows, J.P.; Schneider, W.; Geary, J.C.; Chance, K.V.; Goede, A.P.H.; Aarts, H.J.M.; de Vries, J.; Smorenburg, C.; Visser, H. Atmospheric Remote Sensing with SCIAMACHY. In *Processing of Digest of Topical Meeting on Optical Remote Sensing of the Atmosphere*, Washington, DC, USA, 1990; pp. 71–74.
30. Burrows, J.P.; Chance, K.V. Scanning imaging absorption spectrometer for atmospheric cartography. *Proc. SPIE*. **1991**, *1490*, 146–155.
31. Buchwitz, M.; De Beek, R.; Noël, S.; Burrows, J.P.; Bovensmann, H.; Bremer, H.; Heimann, M. Carbon monoxide, methane and carbon dioxide columns retrieved from SCIAMACHY by WFM-DOAS: year 2003 initial data set. *Atmos. Chem. Phys.* **2005**, *5*, 3313–3329.

32. Weber, M.; Lamsal, L.N.; Burrows, J.P. Improved SCIAMACHY WFDOAS Total Ozone Retrieval: Steps towards Homogenising Long-Term Total Ozone Datasets from GOME, SCIAMACHY, and GOME2. In Processing of Envisat Symposium 2007, Montreux, Switzerland, 23–27 April 2007; ESA SP–636.
33. Barkley, M.P.; Monks, P.S.; Friess, U.; Mittermeier, R.L.; Fast, H.; Körner, S.; Heimann, M. Comparisons between SCIAMACHY atmospheric CO₂ retrieved using (FSI) WFM-DOAS to ground based FTIR data and the TM3 chemistry transport model. *Atmos. Chem. Phys.* **2006**, *6*, 4483–4498.
34. Reuter, M.; Bovensmann, H.; Buchwitz, M.; Burrows, J.P.; Connor, B.J.; Deutscher, N.M.; Wunch, D. Retrieval of atmospheric CO₂ with enhanced accuracy and precision from SCIAMACHY: Validation with FTS measurements and comparison with model results. *J. Geophys. Res.* **2011**, *116*, D04301.
35. Pagano, T.S.; Aumann, H.H.; Hagan, D.E.; Overoye, K. Prelaunch and in-flight radiometric calibration of the Atmospheric Infrared Sounder (AIRS). *IEEE Trans. Geosci. Remote Sens.* **2003**, *41*, 265–273.
36. Xiong, X.; Barnet, C.; Maddy, E.; Sweeney, C.; Liu, X.; Zhou, L.; Goldberg, M. Characterization and validation of methane products from the Atmospheric Infrared Sounder (AIRS). *J. Geophys. Res.* **2008**, *113*, G00A01, doi:10.1029/2007JG000500, 1–14.
37. Maddy, E.S.; Barnet, C.D.; Goldberg, M.; Sweeney, C.; Liu, X. CO₂ retrievals from the Atmospheric Infrared Sounder: Methodology and validation. *J. Geophys. Res.* **2008**, *113*, D11301.
38. Engelen, R.J.; Serrar, S.; Chevallier, F. Four-dimensional data assimilation of atmospheric CO₂ using AIRS observations. *J. Geophys. Res.* **2009**, *114*, D03303, doi:10.1029/2008JD010739, 1–12.
39. He, Q.; Yu, T.; Cheng, T.H.; Gu, X.F.; Xie, D.H.; Wu, Y. Atmospheric carbon dioxide satellite remote sensing retrieval accuracy inspection and spatio-temporal characteristics analysis. *J. Geo-Info. Sci.* **2012**, *14*, 250–257.
40. Shi, G.Y.; Dai, T.; Xu, N. Latest progress of the study of atmospheric CO₂ concentration retrievals from satellite. *Adv. Earth Sci.* **2010**, *25*, 7–13.
41. Wunch, D.; Toon, G.C.; Blavier, J.F.L.; Washenfelder, R.A.; Notholt, J.; Connor, B.J.; Wennberg, P.O. The total carbon column observing network. *Philos. T. R. Soc. A.* **2011**, *369*, 2087–2112.
42. Washenfelder, R.A.; Toon, G.C.; Blavier, J.F.; Yang, Z.; Allen, N.T.; Wennberg, P.O.; Daube, B.C. Carbon dioxide column abundances at the Wisconsin Tall Tower site. *J. Geophys. Res.* **2006**, *111*, D22305, doi:10.1029/2006JD007154, 1–11.
43. Deutscher, N.M.; Griffith, D.W.T.; Bryant, G.W.; Wennberg, P.O.; Toon, G.C.; Washenfelder, R.A.; Park, S. Total column CO₂ measurements at Darwin, Australia—site description and calibration against in situ aircraft profiles. *Atmos. Meas. Tech.* **2010**, *3*, 947–958.
44. Wunch, D.; Toon, G.C.; Wennberg, P.O.; Wofsy, S.C.; Stephens, R.S.; Fischer, M.K.; Zondlo, M.A. Calibration of the total carbon column observing network using aircraft profile data. *Atmos. Meas. Tech.* **2010**, *3*, 1351–1362.
45. Messerschmidt, J.; Geibel, M.C.; Blumenstock, T.; Chen, H.; Deutscher, N.M.; Engel, A.; Xueref-Remy, I. Calibration of TCCON column-averaged CO₂: The first aircraft campaign over European TCCON sites. *Atmos. Chem. Phys.* **2011**, *11*, 10765–10777.

46. Andrews, A.E.; Boering, K.; Daube, B.C.; Wofsy, S.C.; Loewenstein, M.; Jost, H.; Strahan, S.E. Mean ages of stratospheric air derived from in situ observations of CO₂, CH₄, and N₂O. *J. Geophys. Res.* **2001**, *106*, 32295–32314.
47. Messerschmidt, J.; Macatangay, R.; Notholt, J.; Petri, C.; Warneke, T.; Weinzierl, C. Side by side measurements of CO₂ by ground-based Fourier transform spectrometry (FTS). *Tellus B.* **2010**, *62*, 749–758.
48. Sussmann, R.; Rettinger, M.; Borsdorff, T. The new TCCON-FTS site at Garmisch, Germany (47°N, 11°E, 744 m a.s.l.): Set up, first year of operation, and contribution to OCO and GOSAT validation. Proceedings of EGU General Assembly Conference, Vienna, Austria, 19–24 April 2009; 8780.
49. Ohyama, H.; Morino, I.; Nagahama, T.; Machida, T.; Suto, H.; Oguma, H. Column-averaged volume mixing ratio of CO₂ measured with ground-based Fourier transform spectrometer at Tsukuba. *J. Geophys. Res.* **2009**, *114*, D18303, doi:10.1029/2008JD011465, 1–17.
50. Wang, D.Y.; Stiller, G.P.; von Clarmann, T.; Fischer, H.; López-Puertas, M. Cross-validation of MIPAS/ENVISAT and GPS-RO/CHAMP temperature profiles. *J. Geophys. Res.* **2004**, *109*, D19311.
51. Barkley, M.P.; Monks, P.S.; Engelen, R.J. Comparison of SCIAMACHY and AIRS CO₂ measurements over North America during the summer and autumn of 2003. *Geophys. Res. Lett.* **2006**, *33*, L20805.
52. Wunch, D.; Wennberg, P.O.; Toon, G.C.; Connor, B.J.; Fisher, B.; Osterman, G.B. A method for evaluating bias in global measurements of CO₂ total columns from space. *Atmos. Chem. Phys. Discuss.* **2011**, *11*, 20899–20946.
53. Reuter, M.; Buchwitz, M.; Schneising, O.; Heymann, J.; Bovensmann, H.; Burrows, J.P. A method for improved SCIAMACHY CO₂ retrieval in the presence of optically thin clouds. *Atmos. Meas. Tech.* **2010**, *3*, 209–232.